JACS
JOURNAL OF THE AMERICAN CHEMICAL SOCIETY

Article

pubs.acs.org/JACS

Site-Specific Coupling of Hydration Water and Protein Flexibility Studied in Solution with Ultrafast 2D-IR Spectroscopy

John T. King and Kevin J. Kubarych*

Department of Chemistry, University of Michigan, 930 North University Avenue, Ann Arbor, Michigan 48109, United States

Supporting Information

ABSTRACT: There is considerable evidence for the slaving of biomolecular dynamics to the motions of the surrounding solvent environment, but to date there have been few direct experimental measurements capable of site-selectively probing both the dynamics of the water and the protein with ultrafast time resolution. Here, two-dimensional infrared spectroscopy (2D-IR) is used to study the ultrafast hydration and protein dynamics sensed by a metal carbonyl vibrational probe covalently attached to the surface of hen egg white lysozyme dissolved in D_2O/glycerol solutions. Surface labeling provides direct access to the dynamics at the protein−water interface, where both the hydration and the protein dynamics can be observed simultaneously through the vibrational probe's frequency−frequency correlation function. In pure D_2O, the correlation function shows a fast initial 3 ps decay corresponding to fluctuations of the hydration water, followed by a significant static offset attributed to fluctuations of the protein that are not sampled within the <20 ps experimental window. Adding glycerol increases the bulk solvent viscosity while leaving the protein structurally intact and hydrated. The hydration dynamics exhibit a greater than 3-fold slowdown between 0 and 80% glycerol (v/v), and the contribution from the protein's dynamics is found to slow in a nearly identical fashion. In addition, the magnitude of the dynamic slowdown associated with hydrophobic hydration is directly measured and shows quantitative agreement with predictions from molecular dynamics simulations.

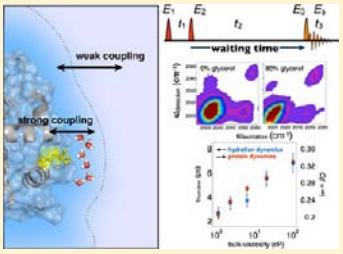

INTRODUCTION

In solution, proteins are not defined by single static structures, but are instead dynamic, continually sampling various local and global conformations.[1−3] Protein fluctuations extend over many time scales, ranging from side-chain motion and low-frequency normal modes that fluctuate on tens of picoseconds, to domain rearrangements that can occur on the time scale of microseconds and longer.[2,4] Time-resolved photolysis experiments,[5−7] temperature-dependent neutron scattering experiments,[8−13] and ultrafast vibrational spectroscopy[14,15] have demonstrated that the fluctuations of the protein are, to some extent, coupled to the fluctuations of the solvent. As a result, the interfacial region between the protein and the hydration water could play a significant role in defining the dynamic character of a protein.

The interest in the protein−water interface has motivated efforts to develop experimental techniques capable of accessing this key region notoriously difficult to study directly.[16−22] Several spectroscopic methods, such as NMR,[16,17] EPR,[18] time-resolved fluorescence upconversion,[19,20] terahertz absorption,[21] and two-dimensional infrared spectroscopy,[22] have been implemented to study the protein−water interface with site-specific resolution. Much of the work has focused on characterizing the influence of extended hydrophobic surfaces on the dynamics of the surrounding water through the hydrophobic effect.[23−26] These experimental methods can also provide a complement to neutron scattering experiments by gaining site-specific information regarding the coupling of protein dynamics to dynamical fluctuations of the solvent.

In addition to gaining site-specific information, spectroscopic techniques also allow for protein dynamics to be studied in dilute solutions at protein concentrations of ∼mM. Many neutron scattering and Mössbauer spectroscopy experiments are carried out on hydrated protein powders, with hydration levels, h, of 0.1−1.0 (h is defined as the mass ratio of water to protein). While these experiments have been valuable in systematically investigating protein flexibility as it gains a full hydration shell, there are potential influences from protein−protein interactions and crowding effects that could contribute to the observed dynamics. For example, recent neutron scattering experiments on concentrated solutions of lysozyme in D_2O/LiCl mixtures indicate that the degree of protein−solvent coupling may be influenced by the relative concentrations of protein and water.[27] 2D-IR spectroscopy using strong vibrational probes can alleviate these potential complications by studying the proteins in dilute solutions, free from any influences of crowding effects.[14,15,22]

We have recently developed a vibrational labeling technique based on a metal carbonyl adduct first identified and characterized by Santos-Silva et al.[28] that provides a unique perspective into ultrafast dynamics at the protein−water interface. In this study, we use 2D-IR spectroscopy to measure the dynamics of hen egg white lysozyme (HEWL) labeled with a ruthenium dicarbonyl (labeled complex referred to as HEWL-RC) attached to the His15 residue (Figure 1). The probe

Received: July 27, 2012
Published: October 26, 2012

dx.doi.org/10.1021/ja307401r | J. Am. Chem. Soc. 2012, 134, 18705−18712

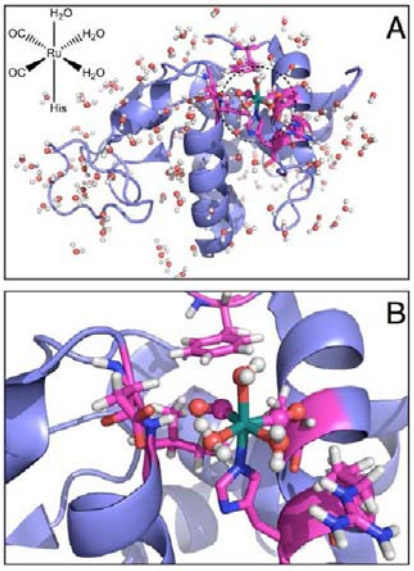

Figure 1. (A) Crystal structure of the HEWL-RC complex showing the most prominent binding location of the vibrational probe [PDB: 2XJW]. The structure is shown with the crystallographic water. (B) Local binding of the vibrational probe to the His15 location.

consists of a ruthenium center coordinated to the His15 residue with three aqua ligands and two carbonyl (C≡O) ligands, which serve as the vibrational probes. To alter the bulk solvent dynamics, we investigated the labeled enzyme in pure D_2O and in D_2O/glycerol mixtures. Early work by Klibanov et al. demonstrated that correct protein folding and function could be achieved in nearly anhydrous solutions of glycerol,[29] suggesting that protein surfaces can efficiently exclude glycerol, remaining fully hydrated with only small amounts of water present. Neutron scattering experiments on concentrated solutions of lysozyme in H_2O/glycerol mixtures have also shown that lysozyme remains mostly hydrated in the prescence of glycerol.[30] The ability to systematically change the bulk-solvent viscosity through the addition of glycerol while leaving the protein structurally stable makes this an excellent model system to study site-specific protein−solvent coupling.

The interfacial dynamics are observed through the frequency−frequency correlation function (FFCF), which is extracted from 2D-IR spectra recorded for the HEWL-RC complex in mixtures ranging from pure D_2O to 80% (v/v) D_2O/glycerol. In the condensed phase, the transition frequency of a vibrational chromophore is modulated by various microenvironments of the solvent around the probe, seen in the linear IR spectrum as an inhomogeneously broadened line shape. Ultrafast 2D-IR spectroscopy enables direct observation of the time scales on which these microenvironments exchange through the decay of the FFCF.[31−35] The numerous configurations of the hydration environment and protein conformations contribute to the inhomogeneous broadening of the CO chromophore, and therefore the water and protein fluctuations are both contained in the decay of the FFCF. The separation of time scales for the fast hydration dynamics and the slow protein dynamics allows these two contributions to be studied independently. Because the water motion occurs on time scales directly accessed in the experiment, the dynamics of the hydration shell appears as a fast decay of the FFCF. Motions of individual protein domains, however, occur on time scales not sampled directly in the experimental window and thus contribute static offsets to the FFCFs, indicating that the spectral inhomogeneity is not completely sampled during the experiment.[36−38] The influence of glycerol on the hydration dynamics and protein fluctuations can thus be observed simultaneously.

RESULTS AND DISCUSSION

Accessing Water Dynamics with Vibrational Probes. In these experiments, the dynamics of water are accessed through the spectral dynamics of metal−carbonyl vibrational probes. We rely on comparisons between two small metal carbonyl molecules, CORM-2 ($[RuCl_2(CO_3)]_2$) and PI-CORM ($[CO]Fe[N_5C_{22}H_{21}]$),[39] which provide a benchmark for bulk-like water dynamics, and hen egg white lysozyme labeled with a metal−carbonyl vibrational probe (Figure 1). The FFCFs of CORM-2 and PI-CORM decay completely with time constants of 1.5 ± 0.3 and 1.6 ± 0.4 ps, respectively (Figure 2). This time scale is expected for bulk-like D_2O and

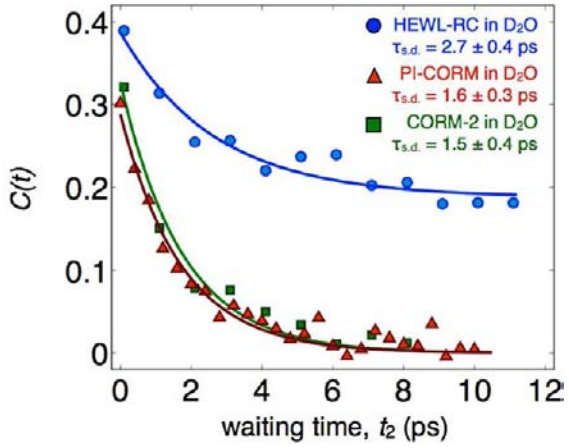

Figure 2. Spectral diffusion of HEWL-RC as compared to spectral diffusion of CORM-2 and PI-CORM in pure D_2O, showing an experimentally determined slowdown factor of 1.8. This is in excellent agreement with molecular dynamics simulations of Laage et al.,[48] which predict a dominant slowdown factor of 2 based on the restriction of hydrogen-bond switching events.

reflects the hydrogen-bonding dynamics of the hydrating heavy water.[40,41] The complete decay of the correlation function around the small hydrophobic molecules demonstrates that a single, small hydrophobe does not significantly influence the dynamics of the hydrating water.[42] The insensitivity of the spectral diffusion time scales to the chemical structures of the vibrational probes indicates that spectral diffusion measurements in aqueous environments are robust sensors of the surrounding environment. Additionally, the apparent invariance to structure enables direct comparisons between various probe molecules.

There have been many ultrafast experiments that are aimed at studying hydration dynamics around hydrophobic molecules/surfaces directly through the OH/OD stretch. These experiments have provided valuable information regarding the behavior of water in isolated pools or in solutions with high concentrations of hydrophobes.[43−47] Studying hydration dynamics through the use of strong vibrational probes provides a complementary view by allowing water to be studied around isolated small molecules or proteins that are in low concentrations, free from possible crowding effects.[42] Studying

dx.doi.org/10.1021/ja307401r | J. Am. Chem. Soc. 2012, 134, 18705−18712

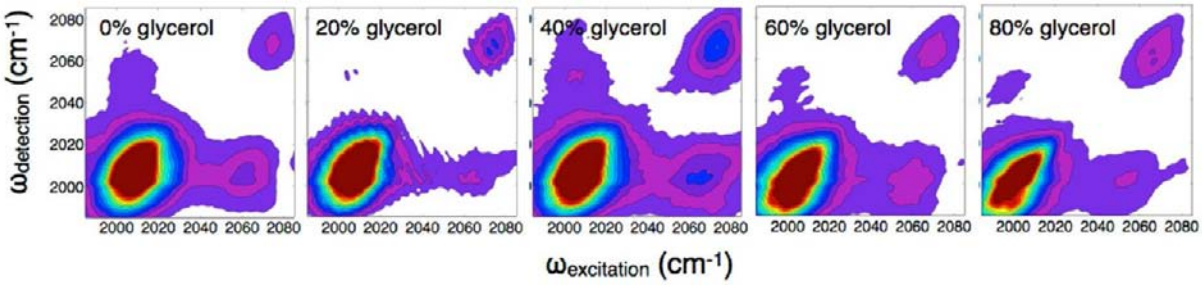

Figure 3. 2DIR absolute value rephasing spectra of HEWL-RC in D_2O/glycerol mixtures. The waiting time between pump pulses and probe pulses, t_2, is 500 fs for all spectra.

hydration dynamics at sub-millimolar solute concentrations provides direct access to the influence of isolated hydrophobes on the surrounding water, whereas similar studies investigating the water itself are virtually impossible due to the several orders of magnitude imbalance between solvating and bulk water molecules.

Magnitude of Constrained Water Slowdown at the Protein Surface. There is still a considerable debate regarding the origin and magnitude of the slowdown of water near hydrophobic molecules and surfaces. Recent experimental and theoretical studies have suggested that the origin of the hydrophobic effect is the limiting of hydrogen-bond switching events near hydrophobic surfaces through an excluded volume effect.[22,42,48] Furthermore, molecular dynamics simulations of HEWL in water have suggested that the magnitude of hydrogen-bond switching slowdown is roughly a factor of 2 relative to bulk water for the large majority of hydrating waters.[48] To experimentally compare more quantitatively the dynamics of bulk water and hydrophobic hydration water, we use the measured spectral diffusion times of CORM-2 and PI-CORM in D_2O, which were found to be 1.5 ± 0.3 and 1.6 ± 0.4 ps, respectively (Figure 2), indicative of bulk hydration. In contrast to these small molecule solutes, the correlation function of the HEWL-RC system exhibits two distinct features: an initial decay corresponding to the hydration dynamics, and a static offset corresponding to protein dynamics that are too slow to be sampled during the experimental window. The fast decay time of the FFCF of HEWL-RC in D_2O decays on the order of 2.7 ± 0.4 ps, which is only modestly slower than bulk-like water (measured as 1.5 ps). The experimentally measured slowdown factor of roughly 1.8 is in excellent quantitative agreement with molecular dynamics simulations.[48] The agreement between experiment and simulations lends support not only to the methodology of studying protein hydration with multidimensional spectroscopy, but also to the interpretation of hydrophobic hydration as resulting from hindered hydrogen-bond switching events due to excluded volume effects.

Modulating Hydration and Protein Dynamics with Cosolvents. To further expand this method of studying the hydration environments of proteins with site-specific resolution, we attempt to modulate and further constrain the hydration water around HEWL using a kosmotropic cosolvent, glycerol. It is known from neutron scattering experiments[8,30,49] and thermodynamic data[50,51] that glycerol is preferentially excluded from the protein surface at nearly all concentrations. As a result, the protein structure and first hydration shell are preserved in the presence of glycerol, which acts to increase the viscosity of the bulk solvent without altering the immediate chemical environment. This cosolvent approach provides an excellent platform for studying the coupling of protein and hydration dynamics to the bulk solvent.

Solvent-Dependent Linewidths and Vibrational Relaxation. The 2D-IR spectra and linear FTIR spectrum of HEWL-RC in D_2O/glycerol mixtures are shown in Figures 3 and 4A,

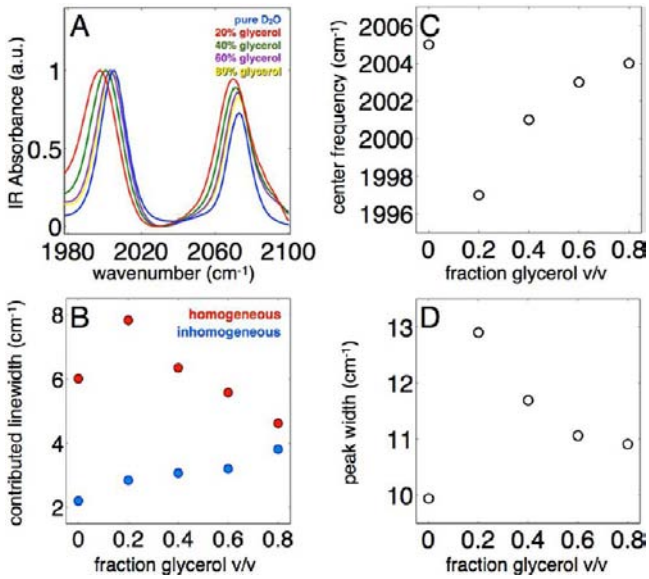

Figure 4. (A) FTIR spectra of HEWL-RC in pure D_2O and D_2O/glycerol mixtures. The main observations in the linear spectrum are the center frequencies of the low-frequency mode (C) and the peak widths of the low-frequency mode (D). The peak width measured in linear FTIR spectroscopy contains contributions from homogeneous and inhomogeneous broadening. 2D-IR spectroscopy allows these contributions to be separated using the fwhm of the linear spectrum and the $C(t = 0)$ value of the FFCF (B).

respectively. Because of the stronger signal strength in the 2D-IR spectrum, the low-frequency mode is analyzed. From the linear spectrum, the center frequency and the peak width (fwhm) of the low-frequency transition were determined. Using the linear and 2D-IR spectra together, the homogeneous and inhomogeneous contributions to the total line width were extracted using a procedure introduced by Kwak et al.[32] The homogeneous line width shows a sharp increase at low glycerol concentrations, followed by a steady decrease. The decrease in linewidths corresponds to slower dephasing times, which reflects an increase in local viscosity induced by higher concentrations of glycerol. The inhomogeneous contribution is found to increase only slightly over the entire range of mixtures. The increase in inhomogeneous broadening of the

dx.doi.org/10.1021/ja307401r | J. Am. Chem. Soc. 2012, 134, 18705−18712

CO transitions reflects a larger configurational space being sampled by the local region of the protein surrounding the vibrational chromophore.

2D-IR spectra were recorded for HEWL-RC in pure D_2O as well as in D_2O/glycerol mixtures (20%, 40%, 60%, 80% glycerol by volume) for t_2 waiting times of 0−11 ps with 1 ps steps. The previously reported sub-5 ps relaxation of the CO vibrations in water and heavy water limits the observational window.[22,52] Our previous work on HEWL-RC in mixtures of D_2O and 2,2,2-trifluoroethanol (TFE) found that the dehydration of the protein surface results in a pronounced increase in the carbonyl label's vibrational lifetime.[22] In the solvent mixtures, the vibrational lifetime of the 2004 cm^{-1} mode was found to be insensitive to the addition of glycerol, which provides consistent, yet novel, confirmation that glycerol is indeed preferentially excluded from the protein surface (Figure 5), and that the protein remains solvated by water.

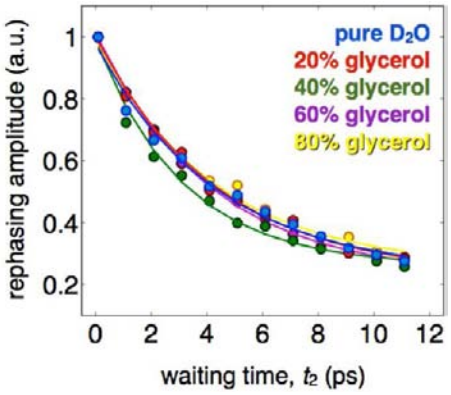

Figure 5. (A) Vibrational relaxation of the low-frequency mode extracted from the rephasing spectrum. The vibrational lifetimes are faster than 5 ps for all solvent compositions, suggesting that the region of the vibrational probe remains largely hydrated despite the presence of the cosolvent.

Spectral Dynamics of HEWL-RC in D_2O/Glycerol Mixtures. Figure 6A shows the FFCF for the 2004 cm^{-1} mode of HEWL-RC in pure D_2O. The two distinguishing features in the correlation function are a fast initial decay and a significant static offset. Again, the fast decay occurs on a 2.7 ps time scale, corresponding to the hydration dynamics. The static offset of the correlation function results from inhomogeneities arising from protein conformations that fluctuate on the time scale of tens of picoseconds or longer, and hence appear static on the time scale accessible within the vibrational lifetime of the probe.[36−38] Although the protein contribution is not time-resolved and appears only as a static offset, the large difference in time scales between the hydration dynamics and the protein conformational dynamics allows both to be measured simultaneously. While the observed vibrational lifetimes suggest that glycerol does not directly interact with the protein surface, the measured spectral diffusion shows pronounced changes upon the addition of glycerol (Figure 6B). The time scale of the fast decay as a function of bulk solvent viscosity is shown in Figure 6C. The viscosity of D_2O/glycerol mixtures was calculated using a kinematic model and follows a viscosity trend similar to that of H_2O/glycerol mixtures that have been measured experimentally (Supporting Information). This observation shows that glycerol indirectly influences the hydration dynamics without leading to dehydration of the protein surface. Furthermore, the protein flexibility is clearly hindered in a nearly identical manner (Figure 6C).

Despite evidence that there is little mixing between the hydration water and the bulk-solvent, both the protein and the hydration water are linked to the dynamics of the bulk solvent. The time scales of the spectral diffusion caused by the hydration environment increase more than 3-fold, ranging from 2 to 7 ps over a bulk viscosity range of 1−120 cP. We note that previous studies observing spectral diffusion of a small metal carbonyl complex in alcohol solvents yielded a similar change in spectral diffusion time scales, but required a much smaller viscosity range (1−4 cP).[34] The relatively weak coupling of the hydration dynamics to the bulk viscosity is not unexpected given the inhomogeneous nature of the solvation environment, which gradually transitions from pure water at the protein surface to a homogeneous bulk solution. In addition, dynamical decoupling from solvent dynamics can become accentuated at sufficiently high viscosities, which has been observed with molecular reorientation[53] as well as dynamics in fragile glasses.[35]

Side-chain motions are often observed in proteins as a decay of the FFCF on the time scale of tens of picoseconds.[54,55] Here, we do not observe any indication of side-chain motions contributing to the decay of the correlation functions, which are accurately fit using a single exponential decay and a static offset. Recent NMR relaxation results have found that the side chains of HEWL show unusually rigid dynamics[56] as compared to

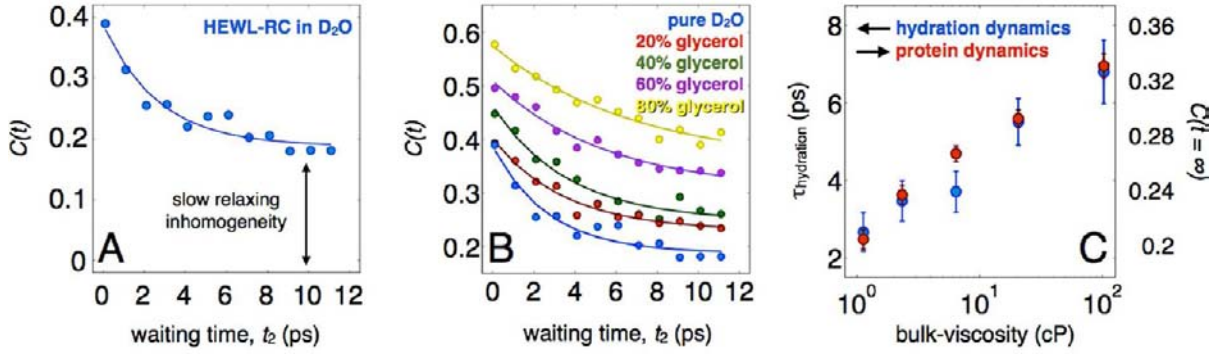

Figure 6. (A) FFCF of HEWL-RC in pure D_2O, highlighting the initial decay due to hydration dynamics and the static offset of the correlation function corresponding to the protein dynamics. (B) Correlation functions for each solvent composition, ranging from pure D_2O to 80% glycerol by volume. From the data, it is clear that there is a marked slowing in the hydration dynamics as well as in the protein dynamics (C).

dx.doi.org/10.1021/ja307401r | J. Am. Chem. Soc. 2012, 134, 18705−18712

what is more traditionally observed in protein backbone[57] and side-chain motions.[58] The rigidity of HEWL is also suggested from thermodynamic data.[59] The rigidity of the side-chain dynamics of HEWL could certainly limit the contribution of side-chain dynamics to the FFCF. In addition, the crystal structure of HEWL-RC shows that the CO oscillators are in the immediate vicinity of isoleucine, phenylalanine, and alanine residues, which are nonpolar side chains that would not likely strongly influence the transition frequency of the CO units. The nonpolar local protein environment experienced by the vibrational probe, together with the rigidity of the side-chain motions in HEWL, likely lead to the absence of side-chain contributions in the FFCF. While the side-chain motions are not observed in the spectral dynamics, the main conclusions of the present work regard the more global fluctuations of the protein, and the coupling of these motions to the hydration water and the bulk solvent. The restricted dynamics of HEWL prevents a more complete picture of protein−solvent coupling that would extend to local side-chain motions, although this information is in principle available using the presented methodology. Our ultrafast 2D-IR results, combined with NMR relaxation observables, suggest that NMR relaxation studies of HEWL in glycerol/water solutions would help to bridge the time scales intrinsic to these two complementary methods.

Calorimetric data have shown that lysozyme undergoes only modest changes in conformational entropy over the glycerol range studied here. Significant changes to the structural ensemble are only induced at higher concentrations,[51] where the structures converge to a narrower ensemble. The observed trend in the static component of the correlation function is thus attributed mostly to a dynamical effect, where the time scales for sampling conformational substates within an ensemble of configurations are modulated by the addition of glycerol. This picture is supported by the nearly constant inhomogeneous spectral width at all glycerol concentrations (Figure 2B).

Without the aid of molecular dynamics simulations, it is difficult to assign the protein motions that are being influenced by the presence of the cosolvent, but in general, protein motion is known to occur on several time scales. Because the protein's contribution is so sensitive to glycerol concentration, it is probable that the motions most susceptible to the solvent occur on time scales just outside the experimental window, and thus can have a significant influence on the FFCF. The hinge-like modes of lysozyme, for instance, are characterized by frequencies of a few wavenumbers, corresponding to periods of 10−30 ps.[4,60] The rigidity of HEWL likely helps increase the frequency of the hinging-like modes, pushing them closer to the experimental window, and thus makes our measurements particularly sensitive to these global motions. These motions can significantly modulate the frequency of the vibrational probe, which is located at an interface between domains that exhibit opposite displacements when viewed as normal modes (see the Supporting Information for more details).

Site-Specificity and Normal Mode Analysis Suggests Protein−Solvent Coupling "Susceptibility". The His15-bound probe is located at the interface between two helical domains that for some of the low-frequency modes exhibit displacements corresponding to an opening-and-closing of the tertiary contact (Figure 7). From the results of an elastic network normal-mode analysis (NMA),[61] we analyzed the relative motions of the α-carbons in each of the first five normal modes using the α-carbon of His15 as an origin. The NMA output

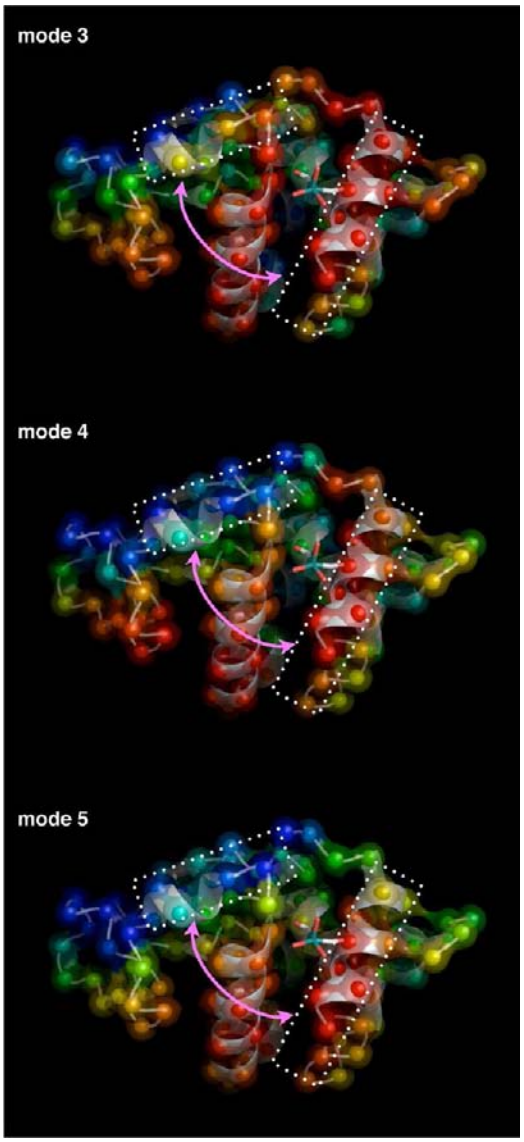

Figure 7. HEWL-RC from PDB file 2XJW showing the metal carbonyl label, color-coded according to the orientational overlap defined in the text. Red corresponds to motion in the same direction as that of His15, blue is in the opposite direction, and other colors are intermediate overlaps. The three modes that have the most pronounced opening-and-closing character at the His15 label site are shown. Dotted areas correspond to the domains that open and close.

consists of a set of coordinates for the α-carbons displaced along the normal mode from the initial structure, so taking the difference between the final and initial positions for α-carbon j results in a net displacement vector $\vec{d}_j$. In addition to the amplitude of motion given by the magnitude of this vector (see the Supporting Information for more details), it is possible to use the set of displacement vectors to map the relative displacement "overlap" as follows. We assign the orientational overlap between α-carbon j and His15 as:

$$\sigma_{j,\mathrm{His15}} = \vec{d}_j \cdot \vec{d}_{\mathrm{His15}}$$

which can range from −1 to 1 because we first normalize all of the displacement vectors. A value, for example, of −1 indicates that the residue moves in precisely the opposite direction of that of the motion of His15. This analysis (which is similar to

dx.doi.org/10.1021/ja307401r | J. Am. Chem. Soc. 2012, 134, 18705−18712

that used in ref 60) loses the magnitude of motion, but that information is apparent from the magnitude. The map is shown in Figure 7 for modes 3, 4, and 5, which showed the largest His15 displacements. The color coding in the map ranges from blue (−1) to red (+1). The displacement overlap maps show that for these three modes, the probe is located between two helices that exhibit considerable hinging motion.

The coupling of hydration and protein dynamics suggests that protein motion most susceptible to the solvent involves significant changes in the surface topology because these are necessarily accompanied by solvent reorganization. Hence, the larger amplitude motions, such as those associated with the collective, low-frequency modes, are most susceptible to solvent slaving. On the other hand, local side-chain motion unimpeded by solvent reorganization may show only a modest solvent dependence, if any. Side chains not capable of hydrogen bonding with the hydration water are likely to be particularly insensitive to changes in the hydration dynamics because of the limited coupling. Hence, the motions of the enzyme most susceptible to slaving are precisely those most influential to the catalytic function, including substrate binding and release. Active site slaving has already been observed in numerous rebinding and 2D-IR studies using heme proteins as models.[5,6,14,15] In most heme proteins, where the binding site is buried within the interior of the protein, 2D-IR studies of bound CO ligands show bulk solvent viscosity-dependent spectral dynamics. Lysozyme, like many enzymes, has a surface accessible catalytic cleft, in addition to a well-studied hinging motion that becomes perturbed upon inhibitor binding.[56] Hence, lysozyme, unlike myoglobin, is a more appropriate model system to investigate the specific link between protein dynamics and catalysis, and how both are slaved to the environment. There is already significant evidence that functionally relevant protein motions occur in the absence of substrate,[3] and the present study offers a promising approach to investigate directly the fundamental picosecond dynamics that underlie these intrinsic dynamics. Because the solvent-coupling of the hinging motions of lysozyme is inherently a surface process, where the coupling of the protein dynamics to the solvent is transmitted by the hydration reorganization that is required for the protein motion, surface-specific probes are required to access the dynamics that can influence such protein motions. In the future, the use of surface probes together with probes on the interior, or at the active site, will be able to provide a more complete picture of protein−solvent coupling.

■ CONCLUSIONS

In this work, we observe that the hydration dynamics around small hydrophobic metal−carbonyls reflects bulk-like dynamics, with spectral diffusion time scales measured to be around 1.5 ps. Furthermore, surface labeling of a protein reveals a modest slowdown of roughly a factor of 2 between bulk D_2O and hydrating D_2O, in quantitative agreement with predictions from MD simulations. The retardation is attributed to the collective solvation dynamics becoming slowed due to the hindering of hydrogen-bond switching events by the extended hydrophobic surface of the protein. In addition, as glycerol is added to modulate the hydration and protein dynamics, a 100-fold increase in bulk viscosity (0−80% glycerol) induces only a modest 3-fold slowdown in the hydration dynamics. Accompanying the hydration retardation is a complementary slowdown of the protein dynamics. The results demonstrate a weak coupling between the hydration water and the bulk solvent, but strong coupling between the protein and water dynamics.

The thermodynamic role of glycerol and other glassy solvents as stabilizing osmolytes originates from creating unfavorable protein backbone−solvent interactions, where the protein preferentially excludes glycerol and other kosmotropes from the protein surface.[62] The dynamic consequence is a modest coupling of the protein dynamics to the bulk solvent mediated by the hydration water, which can act to constrain the space of conformational substates and prevent partial unfolding.[8] Limits imposed by the environment on protein motion can have significant implications on processes such as amyloid fibril formation, which often require partial protein denaturation to nucleate.[63]

Determining factors that influence the structure and dynamics of biological catalysts, in particular the role that crowded, inhomogeneous, and complex environments may play, is an active area of research. The development of experimental techniques that provide time-resolved, site-specific information about the dynamics occurring at the surface of biomolecules will be crucial in elucidating the couplings and dynamics that may contribute to protein structure and function. In this first report using a vibrational site label of a dilute enzyme in solution, we have found that a region at the interface of two helical domains of HEWL is susceptible to solvent slaving, and that the hydration water is also slaved to the bulk solution. Since our earlier study of site-specific hydration revealed that hydration water dynamics is itself heterogeneous, here, with only a single site we are able to propose that solvent−protein coupling is also heterogeneous. The combination of surface labeling and 2D-IR spectroscopy, augmented by site-directed mutagenesis, will allow for a detailed mapping of protein−water interfacial dynamics, including a quantitative analysis of the susceptibility of different regions of the protein to solvent fluctuations and slaving. Because this methodology requires mutations to native proteins, structural analysis will be required to characterize any possible structural changes induced by the mutagenesis and labeling procedures. The sensitivity of vibrational chromophores to solvent environments, in particular aqueous environments, makes this approach well suited for describing protein−protein interfaces crucial for protein recognition as well as protein−water−protein encounters central to aggregation and protein−water−lipid assemblies fundamental to membrane association.[64]

■ ASSOCIATED CONTENT

Ⓢ Supporting Information

A detailed description of the materials and methods used in this work, a description of the low-frequency hinge modes of HEWL, and the calculation of the viscosity of D_2O/glycerol mixtures. This material is available free of charge via the Internet at http://pubs.acs.org.

■ AUTHOR INFORMATION

Corresponding Author

kubarych@umich.edu

Notes

The authors declare no competing financial interest.

■ ACKNOWLEDGMENTS

This work was supported by the National Science Foundation (CHE-0748501) and the Camille & Henry Dreyfus Foundation. We are also grateful to Professor Jeremy Kodanko (Wayne State University, jkodanko@chem.wayne.edu) for supplying us with the PI-CORM molecule used in these experiments.[39]

■ REFERENCES

(1) Elber, R.; Karplus, M. *Science* **1987**, *235*, 318−321.
(2) Frauenfelder, H.; Sligar, S. G.; Wolynes, P. G. *Science* **1991**, *254*, 1598−1603.
(3) Henzler-Wildman, K.; Kern, D. *Nature* **2007**, *450*, 964−972.
(4) McCammon, J. A.; Gelin, B. R.; Karplus, M.; Wolynes, P. G. *Nature* **1976**, *262*, 325−326.
(5) Austin, R. H.; Beeson, K. W.; Eisenstein, L.; Frauenfelder, H.; Gunsalus, I. C. *Biochemistry* **1975**, *14*, 5355−5373.
(6) Ansari, A.; Berendzen, J.; Braunstein, D.; Cowen, B. R.; Frauenfelder, H.; Hong, M. K.; Iben, I. E. T.; Johnson, J. B.; Ormos, P.; Sauke, T. B.; Scholl, R.; Schulte, A.; Steinbach, P. J.; Vittitow, J.; Young, R. D. *Biophys. Chem.* **1987**, *26*, 337−355.
(7) Ansari, A.; Jones, C. M.; Henry, E. R.; Hofrichter, J.; Eaton, W. A. *Science* **1992**, *256*, 1796−1798.
(8) Tsai, A. M.; Neumann, D. A.; Bell, L. N. *Biophys. J.* **2000**, *79*, 2728−2732.
(9) Caliskan, G.; Mechtani, D.; Roh, J. H.; Kisliuk, A.; Sokolov, A. P.; Azzam, S.; Cicerone, M. T.; Lin-Gibson, S.; Peral, I. *J. Chem. Phys.* **2004**, *121*, 1978−1983.
(10) Fenimore, P. W.; Frauenfelder, H.; McMahon, B. H.; Young, R. D. *Proc. Natl. Acad. Sci. U.S.A.* **2004**, *101*, 14408−14413.
(11) Frauenfelder, H.; Chen, G.; Berendzen, J.; Fenimore, P. W.; Jansson, H.; McMahon, B. H.; Stroe, I. R.; Swenson, J.; Young, R. D. *Proc. Natl. Acad. Sci. U.S.A.* **2009**, *106*, 5129−5134.
(12) Jansson, H.; Kargl, F.; Fernandez-Alonso, F.; Swenson, J. *J. Chem. Phys.* **2009**, *130*, 205101−13.
(13) Wood, K.; Plazanet, M.; Gabel, F.; Kessler, B.; Oesterhel, D.; Tobias, D. J.; Zaccai, G.; Weik, M. *Proc. Natl. Acad. Sci. U.S.A.* **2007**, *104*, 18049−18054.
(14) Rector, K. D.; Jiang, J. W.; Berg, M. A.; Fayer, M. D. *J. Phys. Chem. B* **2001**, *105*, 1081−1092.
(15) Finkelstein, I. J.; Massari, A. M.; Fayer, M. D. *Biophys. J.* **2007**, *92*, 3652−3662.
(16) Nucci, N. V.; Pometun, M. S.; Wand, A. J. *Nat. Struct. Mol. Biol.* **2011**, *18*, 245−U315.
(17) Nucci, N. V.; Pometun, M. S.; Wand, A. J. *J. Am. Chem. Soc.* **2011**, *133*, 12326−12329.
(18) Armstrong, B. D.; Choi, J.; Lopez, C.; Wesener, D. A.; Hubbell, W.; Cavagnero, S.; Han, S. *J. Am. Chem. Soc.* **2011**, *133*, 5987−5995.
(19) Qiu, W.; Kao, Y.-T.; Zhang, L.; Yang, Y.; Wang, L.; Stites, W. E.; Zhong, D.; Zewail, A. H. *Proc. Natl. Acad. Sci. U.S.A.* **2006**, *103*, 13979−13984.
(20) Zhang, L.; Wang, L.; Kao, Y.-T.; Qiu, W.; Yang, Y.; Okobiah, O.; Zhong, D. *Proc. Natl. Acad. Sci. U.S.A.* **2007**, *104*, 18461−18466.
(21) Grossman, M.; Born, B.; Heyden, M.; Tworowski, D.; Fields, G. B.; Sagi, I.; Havenith, M. *Nat. Struct. Mol. Biol.* **2011**, *18*, 1102−U1113.
(22) King, J. T.; Arthur, E. J.; Brooks, C. L. I.; Kubarych, K. J. *J. Phys. Chem. B* **2012**, *116*, 5604−5611.
(23) Kauzmann, W. *Adv. Protein Chem.* **1959**, *14*, 1−63.
(24) Dill, K. A. *Biochemistry* **1990**, *29*, 7133−7155.
(25) Tanford, C. *Protein Sci.* **1997**, *6*, 1358−1366.
(26) Chandler, D. *Nature* **2005**, *437*, 640−647.
(27) Chu, X.-q.; Mamontov, E.; O'Neill, H.; Zhang, Q. *J. Phys. Chem. Lett.* **2012**, *3*, 380−385.
(28) Santos-Silva, T.; Mukhopadhyay, A.; Seixas, J. D.; Bernardes, G. J. L.; Romao, C. C.; Romao, M. J. *J. Am. Chem. Soc.* **2011**, *133*, 1192−1195.
(29) Rariy, R. V.; Klibanov, A. M. *Proc. Natl. Acad. Sci. U.S.A.* **1997**, *94*, 13520−13523.
(30) Sinibaldi, R.; Ortore, M. G.; Spinozzi, F.; Carsughi, F.; Frielinghaus, H.; Cinelli, S.; Onori, G.; Mariani, P. *J. Chem. Phys.* **2007**, *126*, 235101−9.
(31) Roberts, S. T.; Loparo, J. J.; Tokmakoff, A. *J. Chem. Phys.* **2006**, *125*, 084502−8.
(32) Kwak, K.; Park, S.; Finkelstein, I. J.; Fayer, M. D. *J. Chem. Phys.* **2007**, *127*, 124503−17.
(33) Tucker, M. J.; Gai, X. S.; Fenlon, E. E.; Brewer, S. H.; Hochstrasser, R. M. *Phys. Chem. Chem. Phys.* **2011**, *13*, 2237−2241.
(34) King, J. T.; Baiz, C. R.; Kubarych, K. J. *J. Phys. Chem. A* **2010**, *114*, 10590−10604.
(35) King, J. T.; Ross, M. R.; Kubarych, K. J. *Phys. Rev. Lett.* **2012**, *108*, 7401−7401.
(36) Chung, J. K.; Thielges, M. C.; Fayer, M. D. *Proc. Natl. Acad. Sci. U.S.A.* **2011**, *108*, 3578−3583.
(37) Ghosh, A.; Qiu, J.; DeGrado, W. F.; Hochstrasser, R. M. *Proc. Natl. Acad. Sci. U.S.A.* **2011**, *108*, 6115−6120.
(38) Bandaria, J. N.; Dutta, S.; Nydegger, M. W.; Rock, W.; Kohen, A.; Cheatum, C. M. *Proc. Natl. Acad. Sci. U.S.A.* **2010**, *107*, 17974−17979.
(39) Jackson, C. S.; Schmitt, S.; Dou, Q. P.; Kodanko, J. J. *Inorg. Chem.* **2011**, *50*, 5336−5338.
(40) Loparo, J. J.; Roberts, S. T.; Tokmakoff, A. *J. Chem. Phys.* **2006**, *125*, 194521−13.
(41) Loparo, J. J.; Roberts, S. T.; Tokmakoff, A. *J. Chem. Phys.* **2006**, *125*, 194522−12.
(42) Laage, D.; Stirnemann, G.; Hynes, J. T. *J. Phys. Chem. B* **2009**, *113*, 2428−2435.
(43) Fayer, M. D. *Acc. Chem. Res.* **2012**, *45*, 3−14.
(44) Fenn, E. E.; Wong, D. B.; Giammanco, C. H.; Fayer, M. D. *J. Phys. Chem. B* **2011**, *115*, 11658−11670.
(45) Park, S.; Fayer, M. D. *Proc. Natl. Acad. Sci. U.S.A.* **2007**, *104*, 16731−16738.
(46) Yang, M.; Szyc, L.; Elsaesser, T. *J. Phys. Chem. B* **2011**, *115*, 13093−13100.
(47) Rezus, Y. L. A.; Bakker, H. J. *Phys. Rev. Lett.* **2007**, *99*, 148301−148304.
(48) Sterpone, F.; Stirnemann, G.; Laage, D. *J. Am. Chem. Soc.* **2012**, *134*, 4116−4119.
(49) Vagenende, V.; Yap, M. G. S.; Trout, B. L. *Biochemistry* **2009**, *48*, 11084−11096.
(50) Gekko, K.; Timasheff, S. N. *Biochemistry* **1981**, *20*, 4667−4676.
(51) Spinozzi, F.; Ortore, M. G.; Sinibaldi, R.; Mariani, P.; Esposito, A.; Cinelli, S.; Onori, G. *J. Chem. Phys.* **2008**, *129*, 035101−9.
(52) King, J. T.; Ross, M. R.; Kubarych, K. J. *J. Phys. Chem. B* **2012**, *116*, 3754−3759.
(53) Lee, M.; Bain, A. J.; McCarthy, P. J.; Han, C. H.; Haseltine, J. N.; Smith, A. B.; Hochstrasser, R. M. *J. Chem. Phys.* **1986**, *85*, 4341−4347.
(54) Thielges, M. C.; Chung, J. K.; Fayer, M. D. *J. Am. Chem. Soc.* **2011**, *133*, 3995−4004.
(55) Urbanek, D. C.; Vorobyev, D. Y.; Serrano, A. L.; Gai, F.; Hochstrasser, R. M. *J. Phys. Chem. Lett.* **2010**, *1*, 3311−3315.
(56) Moorman, V. R.; Valentine, K. G.; Wand, A. J. *Protein Sci.* **2012**, *21*, 1066−1073.
(57) Jarymowycz, V. A.; Stone, M. J. *Chem. Rev.* **2006**, *106*, 1624−1671.
(58) Igumenova, T. I.; Frederick, K. K.; Wand, A. J. *Chem. Rev.* **2006**, *106*, 1672−1699.
(59) Garcia-Hernandez, E.; Zubillaga, R. A.; Chavelas-Adame, E. A.; Vazquez-Contreras, E.; Rojo-Dominguez, A.; Costas, M. *Protein Sci.* **2003**, *12*, 135−142.
(60) Brooks, B.; Karplus, M. *Proc. Natl. Acad. Sci. U.S.A.* **1985**, *82*, 4995−4999.
(61) Tirion, M. M. *Phys. Rev. Lett.* **1996**, *77*, 1905−1908.
(62) Street, T. O.; Bolen, D. W.; Rose, G. D. *Proc. Natl. Acad. Sci. U.S.A.* **2006**, *103*, 13997−14002.
(63) Booth, D. R.; Sunde, M.; Bellotti, V.; Robinson, C. V.; Hutchinson, W. L.; Fraser, P. E.; Hawkins, P. N.; Dobson, C. M.;

Radford, S. E.; Blake, C. C. F.; Pepys, M. B. *Nature* **1997**, *385*, 787−793.
(64) Wei, T.; Carignano, M. A.; Szleifer, I. *Langmuir* **2011**, *27*, 12074−12081.